Electric and optical properties of the 90° ferroelectric domain wall in tetragonal barium titanate

2003 J. Phys.: Condens. Matter 15 8927

(http://iopscience.iop.org/0953-8984/15/50/022)

INSTITUTE OF PHYSICS PUBLISHING JOURNAL OF PHYSICS: CONDENSED MATTER

J. Phys.: Condens. Matter **15** (2003) 8927–8940 PII: S0953-8984(03)68786-2

Electric and optical properties of the 90° ferroelectric domain wall in tetragonal barium titanate

H Chaib, F Schlaphof, T Otto and L M Eng[1]

Institute of Applied Photophysics, University of Technology Dresden, D-01062 Dresden, Germany

E-mail: eng@iapp.de

Received 10 September 2003
Published 3 December 2003
Online at stacks.iop.org/JPhysCM/15/8927

Abstract

The electric and optical properties within 90° ferroelectric domain walls of tetragonal barium titanate ($BaTiO_3$) are theoretically examined at room temperature using a microscopic model which is based on the orbital approximation in correlation with the dipole–dipole interaction. We find that when perpendicularly crossing the domain wall, the variation of the spontaneous polarization and refractive indices does not depend on the thickness of the domain wall which varies between 1.5 and 2.5 nm. Moreover, within the domain wall, the refractive indices n_2 and n_3, corresponding to light polarized parallel to the principal axes $\mathbf{y}_p$ and $\mathbf{z}_p$, respectively, exhibit an important transition in which n_2 transforms from the ordinary to the extraordinary state, while n_3 behaves oppositely to n_2.

1. Introduction

Barium titanate ($BaTiO_3$) is one of the best known ferroelectric materials. After the discovery of its ferroelectric properties it was intensively studied as a representative of compounds having a first order ferroelectric phase transition [1] and field reversible spontaneous polarization below the Curie point. $BaTiO_3$ and comparable materials exhibit a sequence of ferroelectric phase transitions: at high temperature, $BaTiO_3$ single crystals are paraelectric, having a cubic structure. On cooling, they undergo successive structural phase transitions [1], all of them being strictly of first order, showing a large thermal hysteresis [2, 3], a remarkable optical anisotropy [4], and a large spontaneous polarization [1, 4], as well as electro-optic [5, 6] and photorefractive activity [7].

In recent years, a number of experimental investigations have been reported which have focused on characterizing the ferroelectric domains and domain walls in $BaTiO_3$ [8–16] as well as in other ferroelectric materials [17–22]. Transmission electron microscopy and

[1] Author to whom any correspondence should be addressed.

0953-8984/03/508927+14$30.00

x-ray spectroscopy as well as scanning force microcopy have been applied though with limited success: in fact, not one of these inspections has yet been able to deliver any experimental data on the physical properties within the 90° and 180° domain walls of $BaTiO_3$. To our knowledge the few data available on the domain wall properties have been deduced from theoretical calculations mainly focusing on the domain wall thickness, the (elastic) domain wall energy [23], or the domain wall structure and character [24]. More recent theoretical work in this respect reports on first principles calculations in order to compute the energy and thickness of ferroelectric domain walls [25]. By using electron holography, Zhang *et al* [26] found that the width of the 90° domain wall in tetragonal $BaTiO_3$ ranges between 15 and 25 Å. Most probably it is this very small thickness which so far has been the main reason for the difficulty in obtaining experimental data on the physical properties within the domain wall.

Here we present a somewhat different theoretical approach for studying the spontaneous polarization and refractive indices within the 90° domain wall of tetragonal 4 mm $BaTiO_3$ single crystals at room temperature. The microscopic model takes into account the anisotropy in the electronic polarizability of all ions within the domain wall and their ionic shifts as well as the crystalline deformations. In fact, the model was initiated for $BaTiO_3$ by Slater in an earlier work [27] in which he computed the Lorentz correction, finding that the large dipole coupling between Ti and O_z ions along the polar axis is the origin of ferroelectricity in this material. The model has considerably been improved since, as needed to explain different physical properties in $BaTiO_3$.

However, the calculation of optical properties has seemed to be under debate so far. Kinase *et al* [28] tried to explain the high optical anisotropy in $BaTiO_3$ by using the same model which failed, leaving a large disagreement both in value and sign between the calculated (0.0191) and the experimental birefringence (−0.06) [29]. Lawless later showed [30] that the reason for failure was due to the electronic polarizability which was assumed to be isotropic. He then proposed to use the experimentally measured values of refractive indices in order to compute this electronic polarizability anisotropy, which was attributed to the oxygen O_z ions only. Nevertheless, Lawless did not explain the origin of the electronic polarizability anisotropy.

Kinase *et al* [31] then added an important improvement to the model by introducing a microscopic view in form of the quantum mechanical orbital approximation. He showed that the local field acting on the constituent ions through the Kerr effect is the origin for the change in the electronic polarizabilities, and that this change contributes to the optical birefringence; the same analysis was used later to discuss the electro-optic effect in $BaTiO_3$ [32]. In fact when expanding the theory, Kinase assumed the electronic polarizability to be isotropic, i.e. $\alpha = p/E$. However, according to the above mentioned work of Lawless it is clear that the electronic polarizability has to be anisotropic: the correct definition thus reads as $\alpha_{kl} = \partial p_k/\partial E_l$, rather than $\alpha = p/E$.

Khatib *et al* [33] repeated the discussion of the electro-optic effect by using the definition which accounts for the anisotropy of the electronic polarizability (i.e. $\alpha_{kl} = \partial p_k/\partial E_l$). This expansion of the quantum orbital model calculation implicitly considers that $\langle x_1^2\rangle = \langle x_2^2\rangle = \langle x_3^2\rangle$ (where $\langle x_k^2\rangle$ represents the average of the square of the k-component of the distance $\mathbf{R}$ from the core to any point of the wavefunction describing the shell of the ion) which is applicable only for spherical orbitals (i.e. s orbitals). Moreover, in the same work, Khatib *et al* used the value of the spontaneous local field calculated by using the isotropic electronic polarizabilities [34], which makes the improvement incomplete at this stage. In general, the local field (or dipole interaction coefficient) is expanded as a function of longitudinal strains Δ_1, Δ_2, and Δ_3 of the unit cell, which holds perfectly for small Δ_i-values ($\sim 10^{-3}$). However, the development leads to a bunch of lengthy equations specifically when shearing of the unit cell has to be considered (see for instance [35]). This made it hard to apply the model to

situations in which shearing effects are involved, or situations where the components in all directions of the local electric field should be considered simultaneously, as is the case when calculating electro-optic coefficients r_{ij} (particularly the r_{42} coefficient) where the induced shearing has to be considered.

In our actual version of the model, we account for all these points which may be summarized as follows:

- expanding the local electric field by considering its components in all directions at once;
- representing the local electric field in a tensorial equation which allows the description of all its components for all ions simultaneously;
- developing the orbital approximation in such a way that we take into account the anisotropy in the electronic polarizability; and
- considering the correlation between the electronic polarizability and the local electric field (since these two magnitudes are mutually dependent).

The model was previously tested in this version for the calculation of bulk properties of single-domain tetragonal $BaTiO_3$ like the ferroelectricity and optical anisotropy, as well as the linear electro-optical coefficients [36, 37]. Furthermore the same model was successfully applied for modelling electric and optical properties of $LiNbO_3$ single crystals [38], and also within 180° ferroelectric domain walls in $BaTiO_3$ [39]. Based on those experiences which agree excellently well with the corresponding experimental data, we initiate here the application of this model to the more complicated 90° ferroelectric domain wall in $BaTiO_3$ at room temperature.

In fact the principal aim of this work is to study the refractive indices within the domain wall rather than the spontaneous polarization itself. The reason for this is recent near-field optical experiments elucidating the local optical properties within domain walls [8]. In order to reach our goal we start by calculating the spontaneous local electric field and electronic polarizabilities of all ions. Then the spontaneous polarization is easily deduced from the last two magnitudes as a side result.

To our knowledge the refractive indices of the domain wall have never been studied so far either theoretically or experimentally. Further motivation for such calculations stems from today's perspectives in applying optical measuring techniques using the optical near field [8] to directly investigate the local absorption properties [40] as well as the chemical nature of bonding within the domain wall via tip-enhanced Raman spectroscopy [41].

The paper is structured as follows: section 2 discusses the dipole–dipole interaction due to the local field acting on the constituent ions taking into account the individual ionic shifts and crystalline deformations. Also a summary on the electronic polarizability of ions in the $BaTiO_3$ unit cell is given for completeness, as well as the basic approach to our quantum mechanical calculation. Section 3 then presents the results of the spontaneous local electric field, the electronic polarizability, the spontaneous polarization, and refractive indices calculated over the 90° domain wall in tetragonal $BaTiO_3$ at room temperature. We clearly differentiate these results for two different widths of the 90° domain wall. This section then also contains the discussion of the above-mentioned findings.

2. Description of the model

As mentioned above the model is based on the dipole–dipole interaction in correlation with the quantum mechanical orbital approximation where every ion is treated as consisting of a single electron and the effectively charged nucleus [36, 37]. The model therefore accounts for the

possible anisotropy in the electronic polarizability and the crystalline deformations, as well as the ionic shifts both in the bulk and over the domain wall.

For uncharged ferroelectric domain walls the latter are of uttermost importance. We therefore write the strains parallel to the pseudo-cubic [100], [010], and [001] directions of the homogeneous single crystal as Δ_1, Δ_2, and Δ_3. The position $\mathbf{u}(^{\tilde{n}}_{i})$ of ion i sitting in the $\tilde{n}(n_x, n_y, n_z)$ unit cell (indices (n_x, n_y, n_z) represent the coordinates of a unit cell in the whole lattice) may then be given as follows:

- If ion i is located in the $(-)$ region

$$\mathbf{u}^{(-)}(^{\tilde{n}}_{i}) = \begin{pmatrix} 1+\Delta_1 & 0 & 0 \\ 0 & 1+\Delta_2 & 0 \\ 0 & 0 & 1+\Delta_3 \end{pmatrix} \cdot \mathbf{u}(^{\tilde{n}}_{i})^0. \tag{1}$$

  $\mathbf{u}^{(-)}(^{\tilde{n}}_{i})$ is expressed in the crystallographic coordinate system ($\mathbb{B}_{g^{(-)}}$) built up by the three orthogonal base vectors $\mathbf{x}_{g^{(-)}}$, $\mathbf{y}_{g^{(-)}}$, and $\mathbf{z}_{g^{(-)}}$ (see figure 1).
- If ion i is located in the $(+)$ region

$$\mathbf{u}^{(+)}(^{\tilde{n}}_{i}) = \begin{pmatrix} 1+\Delta_1 & 0 & 0 \\ 0 & 1+\Delta_3 & 0 \\ 0 & 0 & 1+\Delta_2 \end{pmatrix} \cdot \mathbf{u}(^{\tilde{n}}_{i})^0. \tag{2}$$

  $\mathbf{u}^{(+)}(^{\tilde{n}}_{i})$ is expressed in the crystallographic coordinate system ($\mathbb{B}_{g^{(+)}}$) built up by the three orthogonal base vectors $\mathbf{x}_{g^{(+)}}$, $\mathbf{y}_{g^{(+)}}$, and $\mathbf{z}_{g^{(+)}}$ (see figure 1).

$\mathbf{u}(^{\tilde{n}}_{i})^0$ represents the position in the cubic phase of ion i in unit cell $\tilde{n}$. $\mathbf{u}^{(-)}(^{\tilde{n}}_{i})$ and $\mathbf{u}^{(+)}(^{\tilde{n}}_{i})$ have to be transposed into the crystallophysic coordinate system ($\mathbb{B}_{\mathrm{p}}$) in which calculations are performed. $\mathbb{B}_{\mathrm{p}}$ is built up by the base vectors $\mathbf{x}_{\mathrm{p}}$, $\mathbf{y}_{\mathrm{p}}$, and $\mathbf{z}_{\mathrm{p}}$ as shown in figure 1.

Ion i of unit cell $\tilde{n}$ is located at a distance $\mu(^{\tilde{n}}_{i})$ from the centre of the domain wall:

$$\mu(^{\tilde{n}}_{i}) = \frac{1}{\sqrt{2}} u_2(^{\tilde{n}}_{i}) - \frac{1}{\sqrt{2}} u_3(^{\tilde{n}}_{i}). \tag{3}$$

The distance $\mathbf{r}(^{\tilde{n},\tilde{m}}_{i,j})$ between ion i sitting in unit cell $\tilde{n}$ and ion j which is found in unit cell $\tilde{m}(m_x, m_y, m_z)$ follows as

$$\mathbf{r}(^{\tilde{n},\tilde{m}}_{i,j}) = [\mathbf{u}(^{\tilde{m}}_{j}) - \mathbf{u}(^{\tilde{n}}_{i})] + [\mathbf{s}(^{\tilde{m}}_{j}) - \mathbf{s}(^{\tilde{n}}_{i})], \tag{4}$$

with $\mathbf{s}(^{\tilde{n}}_{i})$ and $\mathbf{s}(^{\tilde{m}}_{j})$ denoting the shifts of ion i of unit cell $\tilde{n}$ and ion j of unit cell $\tilde{m}$, respectively.

The unit cell volume v then becomes

$$v = a_0^3(1+\Delta_1)(1+\Delta_2)(1+\Delta_3), \tag{5}$$

where a_0 denotes the lattice constant in the cubic phase.

As shown in a recent paper devoted to the 180° domain wall in tetragonal $BaTiO_3$ [39], the local field present along the k-direction acting on ion i of unit cell $\tilde{n}$ is the sum over two contributions.

- The first contribution is obtained by solving the following equation:

$$\sum_{j=1}^{5} \sum_{l=1}^{3} S_{kl}(^{\tilde{n}}_{i,j}) E_l^{\mathrm{loc}}(^{\tilde{n}}_{j}) = Q_k(^{\tilde{n}}_{i}), \tag{6}$$

  where $S_{kl}(^{\tilde{n}}_{i,j})$ and $Q_k(^{\tilde{n}}_{i})$ are two tensors calculable by using the crystallographic properties (lattice constants, ionic shifts) and the electronic polarizabilities of the constituent ions.

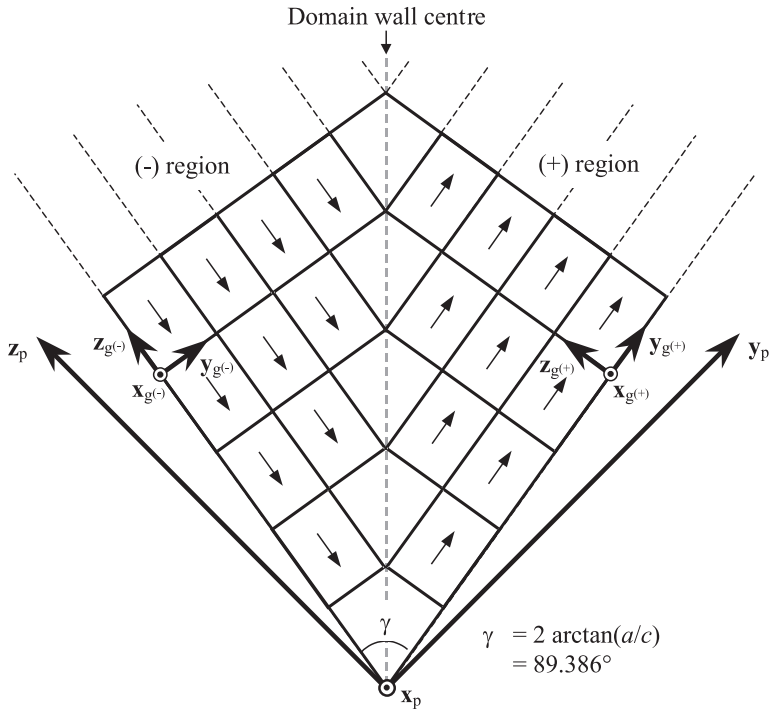

Figure 1. 90° domain wall of tetragonal $BaTiO_3$. γ represents the angle between polarization directions in adjacent ferroelectric domains, being twin components. Arrows show the direction of the spontaneous polarization in each ferroelectric domain.

Expressions for those tensors are given in [39]. The components of the electronic polarizability tensor of ion j in unit cell $\tilde{m}$ are given by [36]

$$\alpha_{k'l}(\tilde{m}_j) = \alpha^{\exp}(j)[\delta_{k'l} - \theta_{k'}(j)\{[E^{\mathrm{loc}}(\tilde{m}_j)]^2\delta_{k'l} + 2E^{\mathrm{loc}}_{k'}(\tilde{m}_j)E^{\mathrm{loc}}_{l}(\tilde{m}_j)\}]. \tag{7}$$

Here $\alpha^{\exp}(j)$ represents the measured free electronic polarizability of ion j. These values are reported in table 1 for completeness, together with the coefficients $\theta_{k'}(j)$. Equation (7) expresses the electronic polarizabilities of the constituent ions of single-domain tetragonal $BaTiO_3$ as a function of their local electric fields [36]. Equation (7) also holds for domain walls as proven in [36]. In brief, to obtain this equation we used the quantum mechanical orbital approximation. This is manifested in treating the electrostatic energy of the core–shell system, introduced by the presence of the local electric field, as a small perturbation within the Schrödinger equation. The quantum mechanical problem is then solved by applying the variational method. As a result we obtain the wavefunctions of the core–shell system in the presence of the electric field, which then in turn are used to compute the components of the electronic polarizability tensor made up from all orbitals involved for one specific ion. Finally, the total electronic polarizability of an ion is obtained by summing over all orbitals.

- The second contribution to the local electric field represents the influence of the local field of ion i of unit cell $\tilde{n}$ in the k-direction due to the variation of the relative dipole moment between unit cell $\tilde{n}$ and unit cell $\tilde{m}$, and is given by [39]

$$\delta E^{\mathrm{loc}}_k(\tilde{n}_i) = \sum_{j=1}^{5}\sum_{k'=1}^{3}\sum_{\tilde{m}} \frac{3r_{k'}(\tilde{n,\tilde{m}}_{i,j})r_k(\tilde{n,\tilde{m}}_{i,j}) - \delta_{kk'}r^2(\tilde{n,\tilde{m}}_{i,j})}{\|\mathbf{r}(\tilde{n,\tilde{m}}_{i,j})\|^5}[p_{k'}(\tilde{n,\tilde{m}}_{i,j}) - p_{k'}(\tilde{n,\tilde{n}}_{i,j})]. \tag{8}$$

Table 1. Measured free electronic polarizabilities $\alpha^{\exp}$ (Å^3) and calculated coefficients θ_k (in10^{-16} esu (CGS units)) of the constituent ions in $BaTiO_3$.

Ion j	$\alpha^{\exp}(j)$	$\theta_1(j)$	$\theta_2(j)$	$\theta_3(j)$
Ba^{2+}	1.9460	39.296	39.296	62.384
Ti^{4+}	0.1859	3.086	3.086	5.718
O^{2-}	2.3940	152.860	152.860	285.850

In the last equation, $\delta_{kk'}$ denotes the Kronecker symbol, and $p_{k'}(^{\tilde{n},\tilde{m}}_{i,j})$ the dipole moment along the k'-direction, which can be expressed as

$$p_{k'}(^{\tilde{n},\tilde{m}}_{i,j}) = \sum_{l=1}^{3} \alpha_{k'l}(^{\tilde{m}}_{j}) E_l^{\mathrm{loc}}(^{\tilde{m}}_{j}) + Z^*_{k'}(j) e [s_{k'}(^{\tilde{m}}_{j}) - s_{k'}(^{\tilde{n}}_{i})]. \tag{9}$$

In equation (9), $Z^*_{k'}(j)$ denotes the effective ionic charge along the k' direction of ion j.

The total polarization $P_k(^{\tilde{n}})$ of the $\tilde{n}$ unit cell is written as

$$P_k(^{\tilde{n}}) = \frac{1}{v} \sum_{j=1}^{5} \left[\sum_{l=1}^{3} \alpha_{k'l}(^{\tilde{m}}_{j}) E_l^{\mathrm{loc}}(^{\tilde{m}}_{j}) + Z^*_k(j) e s_k(^{\tilde{n}}_{j}) \right]. \tag{10}$$

Finally, the connection between the optical dielectric constant $\varepsilon^{\mathrm{opt}}_{kl'}(^{\tilde{n}})$ in unit cell $\tilde{n}$ and the local electric field induced along the l-direction of ion j in unit cell $\tilde{n}$, in the unit of the l'-component of the optical electric field, $\partial E_l^{\mathrm{loc}}(^{\tilde{n}}_{j})/\partial E^{\mathrm{opt}}_{l'}$, is expressed in the following way:

$$\varepsilon^{\mathrm{opt}}_{kl'}(^{\tilde{n}}) = \delta_{kl'} + \frac{4\pi}{v} \sum_{j=1}^{5} \sum_{l=1}^{3} \alpha_{kl}(^{\tilde{n}}_{j}) \frac{\partial E_l^{\mathrm{loc}}(^{\tilde{n}}_{j})}{\partial E^{\mathrm{opt}}_{l'}}. \tag{11}$$

$\partial E_l^{\mathrm{loc}}(^{\tilde{n}}_{j})/\partial E^{\mathrm{opt}}_{l'}$ also consists of two contributions: the first one is obtained by solving the equation

$$\sum_{j=1}^{5} \sum_{l=1}^{3} S_{kl}(^{\tilde{n}}_{i,j}) \frac{\partial E_l^{\mathrm{loc}}(^{\tilde{n}}_{j})}{\partial E^{\mathrm{opt}}_{l'}} = \delta_{kl'}, \tag{12}$$

which is deduced from equation (6). The second contribution is given as follows:

$$\frac{\partial(\delta E_k^{\mathrm{loc}}(^{\tilde{n}}_{i}))}{\partial E^{\mathrm{opt}}_{l'}} = \sum_{j=1}^{5} \sum_{k'=1}^{3} \sum_{\tilde{m}} \frac{3 r_{k'}(^{\tilde{n},\tilde{m}}_{i,j}) r_k(^{\tilde{n},\tilde{m}}_{i,j}) - \delta_{kk'} r^2(^{\tilde{n},\tilde{m}}_{i,j})}{\|\mathbf{r}(^{\tilde{n},\tilde{m}}_{i,j})\|^5} \times \sum_{l=1}^{3} \left(\alpha_{kl}(^{\tilde{m}}_{j}) \frac{\partial E_l^{\mathrm{loc}}(^{\tilde{m}}_{j})}{\partial E^{\mathrm{opt}}_{l'}} - \alpha_{kl}(^{\tilde{n}}_{j}) \frac{\partial E_l^{\mathrm{loc}}(^{\tilde{n}}_{j})}{\partial E^{\mathrm{opt}}_{l'}} \right). \tag{13}$$

The refractive index for light polarized along the k-direction is finally given by

$$n_k = (\eta^{\mathrm{opt}}_{kk})^{-1/2}, \qquad \text{where } \tilde{\eta}^{\mathrm{opt}} = (\tilde{\varepsilon}^{\mathrm{opt}})^{-1}. \tag{14}$$

3. Results and discussion

The calculation of the spontaneous polarization and refractive indices over the 90° domain wall in tetragonal $BaTiO_3$ is carried out for two different domain wall widths at room temperature. The data for the lattice parameters, spontaneous ionic shifts in a homogeneous ideal crystal, and the effective charges used in this calculation are taken from [39]. We assume here that the

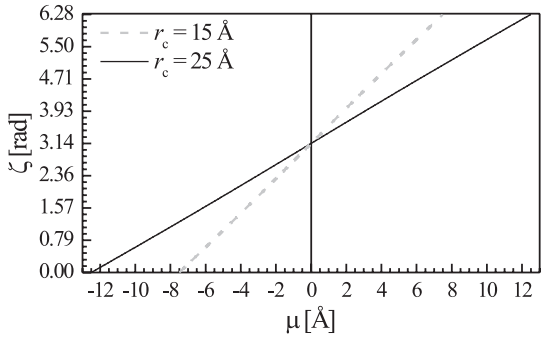

Figure 2. Variation of ζ as a function of distance μ (in algebraic units) from the centre of the domain wall.

components of the effective charges of the constituent ions in the direction of the spontaneous polarization do not change when crossing the domain wall.

Geometrically, we consider the 90° domain wall to coincide with the plane characterized in the bulk by the equation $y = z$ as shown in figure 1. The changes of the spontaneous ionic shifts near the domain wall are given by [42]

$$\begin{aligned} s_1(\tilde{j}^m) &= 0 \\ s_2(\tilde{j}^m) &= (s_3(j))^0 \cos\left(\psi - \frac{\pi}{2}\right) \\ s_3(\tilde{j}^m) &= (s_3(j))^0 \sin\left(\psi - \frac{\pi}{2}\right). \end{aligned} \tag{15}$$

In the last equation, $(s_3(j))^0$, which is the spontaneous ionic shift of ion j in the direction of the spontaneous polarization of a homogeneous ideal crystal, represents the modulus of the order parameter, and $(\psi - \frac{\pi}{2})$ its phase. The phase jump by $-\frac{\pi}{2}$ is introduced in order to account for the difference between our working coordinate system $\mathbb{B}_p$ and that in which the proof of the differential equation (16) governing the variation of ψ was performed by Strukov and Levanyuk in [42]. ψ is obtained by solving the following equation:

$$\frac{d^2\zeta}{d\mu(\tilde{j}^m)^2} - \frac{1}{r_c^2}\sin\zeta = 0, \qquad \text{with } \zeta = 4\psi, \tag{16}$$

where $\mu(\tilde{j}^m)$, given by equation (3), is the distance of ion j of unit cell $\tilde{m}$ from the centre of the domain wall, and r_c represents the width of the domain wall (also known as the correlation radius of the order parameter). To solve the last equation which belongs to the second-order conservative system, we use a numerical algorithm based on Stoermer's rule as expanded in [43], with the boundary conditions $\zeta(-\frac{r_c}{2}) = 0$ and $\zeta(\frac{r_c}{2}) = 2\pi$. To fulfil these conditions, the value of $\frac{d\zeta}{d\mu}|_{\mu=-\frac{r_c}{2}}$ is fitted to $4.083\,38 \times 10^7$ rad cm^{-1} for $r_c = 15$ Å and $2.450\,03 \times 10^7$ rad cm^{-1} for $r_c = 25$ Å. Figure 2 reports these ζ-values as a function of μ for the two domain wall thicknesses $r_c = 15$ and 25 Å. These two bordering values for the 90° domain wall thickness stem from Zhang *et al* [26].

The calculation of the spontaneous local field $\mathbf{E}^{spon}(\tilde{j}^n)$, which corresponds to the value of the local electric field $\mathbf{E}^{loc}(\tilde{j}^n)$ of ion j in unit cell $\tilde{n}$ in the absence of any external electric field ($\mathbf{E}^{ext} = 0$), shows that this spontaneous local electric field does not necessarily have to be aligned along the 3-direction of the crystallophysic coordinate system $\mathbb{B}_p$ for the considered

ion. The reason for this is directly related to the asymmetry of the specific distorted unit cell (and hence the ionic positions). This means that the approximation $\frac{\sum_k E_k^2\langle x_k^2\rangle}{E^2} \simeq \langle x_3^2\rangle$ (see [36] for more detail) is violated in $\mathbb{B}_p$. To remedy the situation, we construct for each ion its own coordinate system $\mathbb{B}_q(\tilde{n}_j)$ for which the $\mathbf{z}_q$-axis is parallel to the spontaneous local electric field of this ion. This coordinate system is built up by the following three orthogonal base vectors: $\mathbf{x}_q(\tilde{n}_j) = (1,0,0)_{\mathbb{B}_p}$, $\mathbf{y}_q(\tilde{n}_j) = (0, \cos\varphi(\tilde{n}_j), \sin\varphi(\tilde{n}_j))_{\mathbb{B}_p}$, and $\mathbf{z}_q(\tilde{n}_j) = (0, -\sin\varphi(\tilde{n}_j), \cos\varphi(\tilde{n}_j))_{\mathbb{B}_p}$. The electronic polarizability is then calculated in this coordinate system, and afterwards transposed into the coordinate system $\mathbb{B}_p$ in which the calculation of all other magnitudes is performed. In fact, the local field of ion j in unit cell $\tilde{n}$ is calculated in $\mathbb{B}_p$ and then transposed to $\mathbb{B}_q(\tilde{n}_j)$ in order to use it for calculating the tensor $\tilde{\alpha}(\tilde{n}_j)$ of this ion. Once this tensor is obtained, we transpose it back to $\mathbb{B}_p$ where it will be used in the calculation for all other magnitudes.

Note that the angle $\varphi(\tilde{n}_j)$, characterizing the $\mathbf{z}_q(\tilde{n}_j)$-vector of $\mathbb{B}_q(\tilde{n}_j)$ relative to the j ion in unit cell $\tilde{n}$, can be evaluated as follows:

- if $\sqrt{(E_2^{\mathrm{loc}}(\tilde{n}_j))^2 + (E_3^{\mathrm{loc}}(\tilde{n}_j))^2} = 0$ then $\varphi(\tilde{n}_j) = 0$;
- if $E_2^{\mathrm{loc}}(\tilde{n}_j) < 0$ then $\varphi(\tilde{n}_j) = \arccos \frac{E_3^{\mathrm{loc}}(\tilde{n}_j)}{\sqrt{(E_2^{\mathrm{loc}}(\tilde{n}_j))^2 + (E_3^{\mathrm{loc}}(\tilde{n}_j))^2}}$;
- if $E_2^{\mathrm{loc}}(\tilde{n}_j) \geqslant 0$ then $\varphi(\tilde{n}_j) = 2\pi - \arccos \frac{E_3^{\mathrm{loc}}(\tilde{n}_j)}{\sqrt{(E_2^{\mathrm{loc}}(\tilde{n}_j))^2 + (E_3^{\mathrm{loc}}(\tilde{n}_j))^2}}$.

From the above relations, it seems that the angle $\varphi(\tilde{n}_j)$ depends on the components of the local electric field which is mutually influenced by the components of the electronic polarizability. This last magnitude is calculated in the $\mathbb{B}_q(\tilde{n}_j)$ coordinate system, which makes it depend on $\varphi(\tilde{n}_j)$. This implicitly means that there exists a mutual dependence between the angle $\varphi(\tilde{n}_j)$ and the components of the local electric field. Thus, a complicated doubly self-consistent calculation has to be performed.

The calculation shows that the values of the spontaneous local electric field acting on the constituent ions of tetragonal $BaTiO_3$ along the 1-direction are exactly zero. On the other hand, values of the two other components of the local electric field $E_{\parallel}^{\mathrm{loc}}(\tilde{n}_j)$ $(=\frac{1}{\sqrt{2}}(E_2^{\mathrm{loc}}(\tilde{n}_j) + E_3^{\mathrm{loc}}(\tilde{n}_j)))$ and $E_{\perp}^{\mathrm{loc}}(\tilde{n}_j)$ $(=\frac{1}{\sqrt{2}}(E_2^{\mathrm{loc}}(\tilde{n}_j) - E_3^{\mathrm{loc}}(\tilde{n}_j)))$ are non-zero and are reported in figure 3 for Ba^{2+}, Ti^{4+}, O_x^{2-}, O_y^{2-}, and O_z^{2-} for the two widths r_c of the domain wall ($r_c = 15$ and 25 Å).

As seen in figure 3, only the Ti^{4+}, O_y^{2-}, and O_z^{2-} ions have important values of the spontaneous local electric field in the $\parallel$- and $\perp$-directions. When crossing the domain wall, the spontaneous local electric field of the Ti^{4+} ion changes its direction without vanishing inside the domain wall. This is because inside the domain wall the $\perp$-direction component $E_{\perp}^{\mathrm{loc}}(Ti^{4+})$ increases by forming a peak centred in the centre of the domain wall while the $\parallel$-direction component $E_{\parallel}^{\mathrm{loc}}(Ti^{4+})$, which is anti-symmetric, measures exactly zero at the centre of the domain wall, with the values to the left and right of the wall having opposite signs. The same behaviour is exhibited by the Ba^{2+} and O_x^{2-} ions with the only difference that the $\perp$-component decreases inside the domain wall instead of increasing. However, the behaviour of the components of the spontaneous local electric field of the ions O_y^{2-} and O_z^{2-} is totally different: the $\parallel$- and $\perp$-components of the spontaneous local electric field of the O_y^{2-} ion, which measure -0.13×10^6 and 0.13×10^6 esu in the $(-)$ region, increase regularly inside the domain wall to achieve the value of 0.92×10^6 esu in the (+) region, while the $\parallel$- and $\perp$-components of the spontaneous local electric field of the O_y^{2-} ion, measuring, respectively, -0.92×10^6 and 0.92×10^6 esu in the $(-)$ region, increase and then decrease inside the domain wall to become 0.13×10^6 esu in the (+) region. Furthermore, in the case of the O_y^{2-} and O_z^{2-}

ions, the ∥-component of the spontaneous local electric field changes its sign without passing through zero as is the case for Ba^{2+}, Ti^{4+}, and O_x^{2-} ions. It thus seems that in the (−) region the value of the spontaneous local electric field of the O_z^{2-} ion is larger compared to the O_y^{2-} ion, and in the (+) region the value of the spontaneous local electric field of the O_y^{2-} ion becomes larger while that of the O_z^{2-} ion becomes weaker. This change can be explained by the fact that in the (−) region the Ti^{4+} ion shifts towards the O_z^{2-} ion and then strongly influences its spontaneous local electric field, while in the (+) region it influences that of the O_y^{2-} ion by shifting towards it. It is noteworthy that the rate of variation of the spontaneous local electric field becomes more important for $r_c = 15$ Å compared to 25 Å.

In single-domain tetragonal $BaTiO_3$, the amplitude of the anisotropy of the electronic polarizability $\delta\alpha(\tilde{n}_j)$ of ion j in unit cell $\tilde{n}$ is defined as the difference between the component of the electronic polarizability in the direction of the polar axis and that in the direction perpendicular to it [36]. This definition does not hold for the 90° domain wall because the direction of the polar axis changes when crossing the wall. However, all elements of the electronic polarizability tensor in the spontaneous state ($\mathbf{E}^{\text{ext}} = 0$) are evaluated by considering equation (7), table 1, and figure 3. The calculation shows that only diagonal elements $\alpha_{kk}(\tilde{n}_j)$ are non-zero. In fact the non-diagonal elements $\alpha_{kl}(\tilde{n}_j)|_{k\neq l}$ are exactly zero outside the domain wall while inside they exhibit a very small change to reach, in the best case, the value of 0.04 $Å^3$ (in absolute units) for α_{23} and α_{32} of $O_{y,z}^{2-}$ ions. This is negligible compared to the value of the free electronic polarizability of the O^{2-} ion (2.394 $Å^3$), or to the value of the anisotropy of the electronic polarizability of the O^{2-} ion calculated in single-domain tetragonal $BaTiO_3$ (0.2858 $Å^3$) [36]. Thus, only the diagonal elements of the electronic polarizability have to be considered. For reasons of clarity we will plot only the electronic polarizability values of the O_y^{2-} and O_z^{2-} ions (see figure 4) since only these ions possess an important anisotropy of the electronic polarizability.

The analysis of these results indicates that for tetragonal $BaTiO_3$ at room temperature, the oxygen O_y^{2-} presents a remarkable anisotropy of the electronic polarizability in the (+) region (figures 4(a) and (c)), while for the oxygen O_z^{2-} a similar anisotropy appears in the (−) region (figures 4(b) and (d)). This anisotropy results in the large difference between the component of the electronic polarizability in the direction of the spontaneous polarization (which is the 3-direction for the (−) region and the 2-direction for the (+) region) and those in the other directions. In fact, in the (−) region, the shift of the Ti^{4+} ion towards the O_z^{2-} ion leads to a strong spontaneous local electric field of the O_z^{2-} pointing along the Ti^{4+}–O_z^{2-} direction which in turn leads to a strong decrease of the component of the electronic polarizability of the O_z^{2-} in the same direction ($\alpha_{33}(O_z^{2-})$) compared to the two other directions $\alpha_{11}(O_z^{2-})$ and $\alpha_{22}(O_z^{2-})$. The same happens in the (+) region for the oxygen O_y^{2-} in the direction Ti^{4+}–O_y^{2-} which leads to a strong decrease of $\alpha_{22}(O_y^{2-})$ compared to $\alpha_{11}(O_y^{2-})$ and $\alpha_{33}(O_y^{2-})$. When crossing the domain wall in the forward direction, the O_y^{2-} diagonal elements α_{kk} of the electronic polarizability decrease and then slightly increase, showing a minimum for $\mu \cong \frac{r_c}{2}$. The decrease is more pronounced for α_{22} compared to α_{11} and α_{33} (see figures 4(a) and (c)). The same scenario holds for the O_z^{2-} ion; however, when crossing the domain wall in the backward direction (i.e. when passing from the (+) region towards the (−) region), the minimum sits at $\mu \cong -\frac{r_c}{2}$, and a large decrease is observed for α_{33} rather than α_{22} as for O_y^{2-} (see figures 4(b) and (d)).

Next we present and discuss the results obtained for the spontaneous polarization in unit cell $\tilde{n}$, $P^{\text{spon}}(\tilde{n})$. $P^{\text{spon}}(\tilde{n})$ is ascribed to the unit cell (and not to the individual ions) and is defined as the total dipole moment (in the unit cell) per volume. The components $P_k(\tilde{n})$ are deduced from equation (10) in the absence of any external field. The calculations show that the values of the spontaneous polarization in tetragonal $BaTiO_3$ at room temperature along the 1-direction are

exactly zero. On the other hand, the values of the two other components of the spontaneous polarization $P_{\parallel}^{\text{spon}}(\tilde{n})$ $\{=\frac{1}{\sqrt{2}}[P_2^{\text{spon}}(\tilde{n}) + P_3^{\text{spon}}(\tilde{n})]\}$ and $P_{\perp}^{\text{spon}}(\tilde{n})$ $\{=\frac{1}{\sqrt{2}}[P_2^{\text{spon}}(\tilde{n}) - P_3^{\text{spon}}(\tilde{n})]\}$ are non-zero and are reported in figure 5, together with $\|\mathbf{P}^{\text{spon}}\|$. We see that the norm of the spontaneous polarization, $\|\mathbf{P}^{\text{spon}}\|$, does not vanish when crossing the domain wall but undergoes an increase before then strongly decreasing towards the centre of the domain wall (at $\mu = 0$). This holds for both widths r_c of the domain wall considered here and also when approaching the domain wall from both sides. However, the component of the spontaneous polarization perpendicular to the domain wall, $P_{\perp}^{\text{spon}}$, which does not exhibit any change outside the domain wall, decreases slightly inside it by forming a negative peak centred in the centre of the domain wall, while the component parallel to the domain wall, $P_{\parallel}^{\text{spon}}$, which is anti-symmetric, undergoes an increase (in absolute units) before then decreasing towards the centre of the domain wall (at $\mu = 0$), also when approaching from both sides. From the above results, we conclude that the spontaneous polarization experiences a rotation accompanied by a change in the norm inside the domain wall. Note that a recent experimental investigation of the 90° domain wall in $BaTiO_3$ by electron holography claimed a pronounced deviation of the measured spontaneous polarization component parallel to the domain wall compared to the hyperbolic tangent function [45].

Figure 6 finally reports the calculated values for the refractive indices n_2 and n_3 ascribed to each unit cell across the domain wall. Note that the calculated results are displayed as discrete values, since the discussion of refractive indices makes physical sense on the unit cell bases only (and not on the ionic scale). Far away from and for any thickness of the domain wall, the crystal possesses only two refractive indices, the ordinary refractive index n_o (which coincides with $n_1 = n_2$ in the (−) region and with $n_1 = n_3$ in the (+) region), and the extraordinary refractive index n_e (which is n_3 in the (−) region and n_2 in the (+) region). The calculated values of these indices are $n_o = 2.3704$ and $n_e = 2.2839$, respectively, which are in good agreement with experimental data ($n_o = 2.398$ and $n_e = 2.312$) given by Johnston and Weingart [5] for single-domain tetragonal $BaTiO_3$ at room temperature.

When approaching the domain wall, however, the three refractive indices become different from each other. Hence the crystal in this region may be characterized as being biaxial, having three different refractive indices. The refractive index n_1 shows a small change when passing through the domain wall, which appears in a single decrease towards $\mu = 0$ for $r_c = 15$ Å, and in a small decrease followed by an increase and a decrease again towards $\mu = 0$ for $r_c = 25$ Å. This fluctuating behaviour can be explained by the fact that unit cells in the centre of the domain wall undergo a very pronounced mechanical deformation which influences their properties (see figure 1). However, the n_2 refractive index, which plays the role of the ordinary refractive index in the (−) region, decreases when crossing the domain wall in the forward direction, and then increases after passing through a minimum located in the (+) region. In this last region, n_2 plays the role of the extraordinary refractive index. On the other hand, the n_3 refractive index, which is the ordinary refractive index in the (+) region rather than the (−) region, decreases when crossing the domain wall in the backward direction and then increases after passing through a minimum located in the (−) region in which n_3 plays the role of the extraordinary refractive index. When crossing the domain wall, the behaviour of n_2 and n_3, which is apparently independent of r_c, may be regarded as a transition in which n_2 and n_3 permutate their role by passing from the ordinary to the extraordinary state and vice versa, respectively.

Our theoretical calculations show that the behaviour of all magnitudes studied here, whether the spontaneous local electric field, the electronic polarizability, the spontaneous polarization, or the refractive indices, is almost the same independent of the domain wall width. The component of the spontaneous polarization parallel to the domain wall, however,

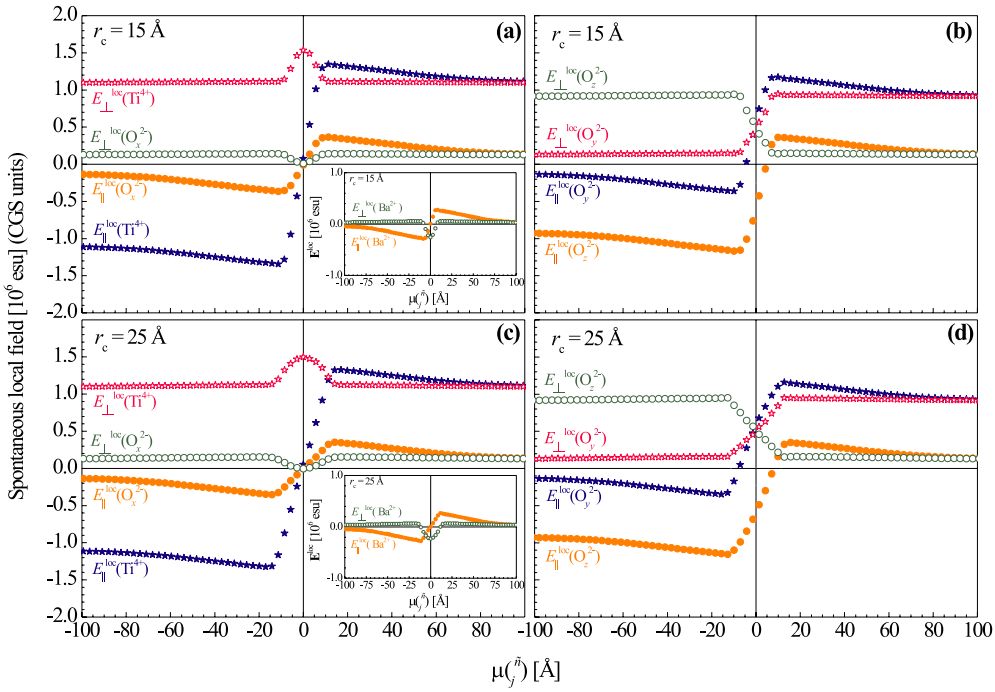

Figure 3. Variation of the ∥- and ⊥-direction components of the spontaneous local field $E^{loc}(\vec{n}_j)$ for Ti^{4+}, O_x^{2-}, O_y^{2-}, and O_z^{2-} when passing through the 90° domain wall of tetragonal $BaTiO_3$. Computation was performed at room temperature with $r_c = 15$ Å (top curves) and $r_c = 25$ Å (bottom curves). Data for the spontaneous local electric field for Ba^{2+} are reported in the insets in (a) and (c).

inverses its sign when passing from the (−) region to the (+) region, having a value of exactly zero at the centre of the domain wall while the perpendicular component always maintains its sign. On the other hand, the refractive indices n_2 and n_3 undergo important changes within the domain wall by passing from the ordinary to the extraordinary state and vice versa, respectively.

4. Conclusions

By using a microscopic model taking into account a quantum method based upon the orbital approximation and the dipole–dipole interaction due to the local field acting on the constituent ions, we calculated the electric and optical properties within 90° ferroelectric domain walls of tetragonal $BaTiO_3$ at room temperature. The calculations show that the spontaneous polarization, spontaneous local electric field, electronic polarizability, and refractive indices hold the same behaviour when changing the domain wall width. However, the spontaneous polarization within the domain wall behaves quite similar to former theoretical work based on a three-dimensional Landau–Ginzburg model [46] and also to recent *ab initio* calculations for the 90° domain wall in tetragonal $PbTiO_3$ [47]. Our model allows us to compute a variety of different microscopic properties both internal and external to the 90° domain wall. Specifically, we find, in contrast to the 180° domain wall, that the anisotropy of electronic polarizability of the oxygen ions as well as the spontaneous polarization holds inside the domain wall without vanishing. Furthermore, the $BaTiO_3$ 90° domain wall behaves like a biaxial crystal, resulting in dramatic changes of the refractive indices n_2 and n_3. Therefore, the optical propagation

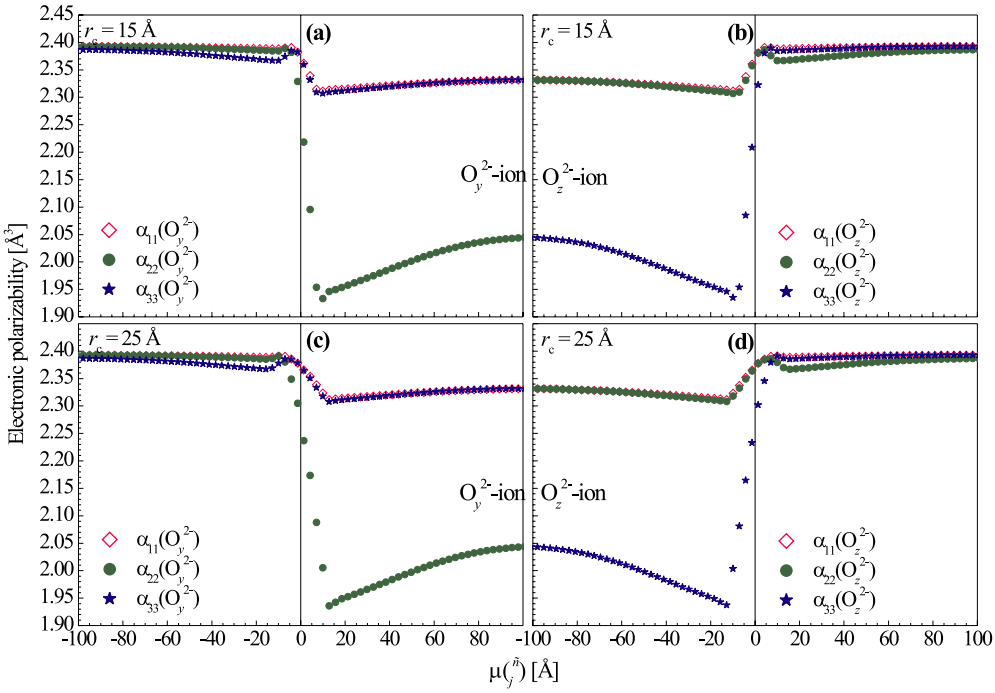

Figure 4. Variation of the diagonal elements of the electronic polarizability of the oxygens O_y^{2-} and O_z^{2-} when passing through the 90° domain wall of tetragonal $BaTiO_3$. Calculations are done at room temperature with $r_c = 15$ Å (top curves) and $r_c = 25$ Å (bottom curves).

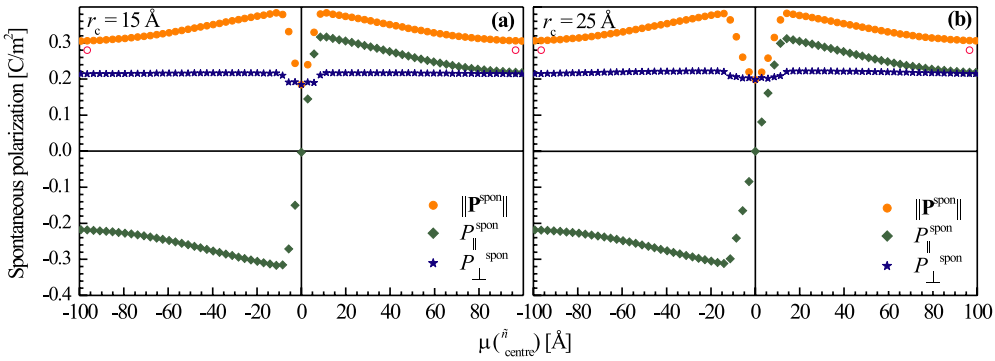

Figure 5. Variation of the norm, $\|\mathbf{P}^{spon}(\tilde{n})\|$, of the spontaneous polarization and its components $P_{\parallel}^{spon}(\tilde{n})$ and $P_{\perp}^{spon}(\tilde{n})$ when crossing the 90° domain wall of tetragonal $BaTiO_3$. Results are computed at room temperature with $r_c = 15$ Å (left) and $r_c = 25$ Å (right). $\mu(\tilde{n}_{centre})$ is the distance (in algebraic units) between the domain wall centre and the unit cell $\tilde{n}$ centre. O represents the experimental value of $\|\mathbf{P}^{spon}\|$ according to Cudney *et al* [44].

properties across such domain walls are expected to experience strong changes affecting the optical transmission specifically for light polarized in the yz-plane. One major driving force to the above mentioned anisotropies might be the oxygen deficiency within the 90° domain wall as recently discovered by aberration corrected TEM [48]. Such effects will be reconsidered in our future investigations.

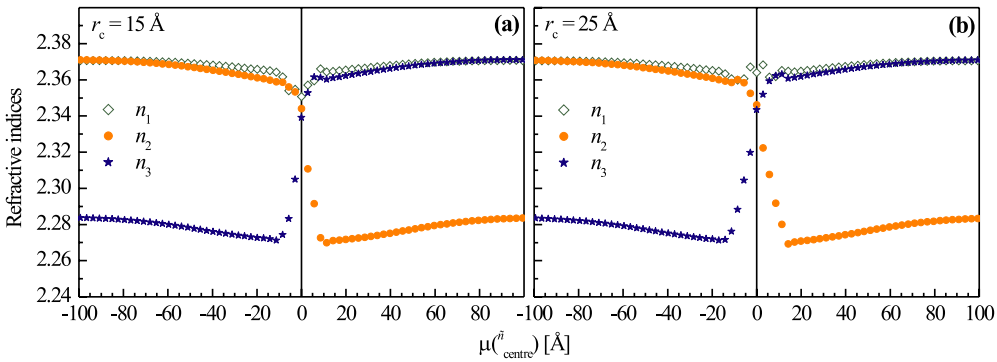

Figure 6. Variation of the refractive indices n_1, n_2, and n_3 when passing through the 90° domain wall of tetragonal $BaTiO_3$. Calculations are done for room temperature with $r_c = 15$ Å (left) and $r_c = 25$ Å (right). $\mu(\tilde{n}_{centre})$ is the distance (in algebraic units) between the domain wall centre and the unit cell $\tilde{n}$ centre.

Acknowledgments

This work was supported by the 'Deutsche Forschungsgemeinschaft' under grant Nos EN 434/2 and EN 434/7.

References

[1] Jona F and Shirane J 1962 *Ferroelectrics Crystals* (New York: Pergamon)
[2] Gonzalo J A, Ramirez R, Lifante G and Koralewski M 1993 *Ferroelectr. Lett.* **15** 9
[3] Noheda B, Karalewski M, Lifante G and Gonzalo J A 1994 *Ferroelectr. Lett.* **17** 25
[4] Line M E and Glass A M 1977 *Principle and Applications of Ferroelectrics and Related Materials* (Oxford: Clarendon)
[5] Johnston A R and Weingart J M 1965 *J. Opt. Soc. Am.* **55** 828
[6] Bernasconi P, Zgonik M and Günter P 1995 *J. Appl. Phys.* **78** 2651
[7] Günter P and Huignard J-P 1988 *Photorefractive Materials and their Applications* ed P Günter and J-P Huignard (Berlin: Springer)
[8] Eng L M, Bammerlin M, Loppacher Ch, Guggisberg M, Bennewitz R, Lüthi R, Meyer E, Heinzelman H and Güntherodt H-J 1999 *Ferroelectrics* **222** 1
[9] Floquet N, Valot C M, Mesnier M T, Niepse J C, Normand L, Thorel A and Kilaas R 1997 *J. Physique* III **7** 1105
[10] Floquet N and Valot C 1999 *Ferroelectrics* **234** 107
[11] Cudney R S, Garces-Chavez G and Nagrete-Regagnon P 1998 *Opt. Lett.* **22** 439
[12] Cudney R S and Kaczmarek M 1999 *Opt. Express* **7** 323
[13] Park B M and Chung S J 1996 *Integr. Ferroelectr.* **12** 275
[14] Park B M, Park H M and Chung S J 1998 *J. Korean Phys. Soc.* **32** S752
[15] Tsunekawa S, Fukuda T, Ozaki T, Yoneda Y, Okabe T and Terauchi H 1998 *J. Appl. Phys.* **84** 999
[16] Eng L M, Abplanalp M and Günter P 1998 *Appl. Phys.* A **66** S679
[17] Lehnen P, Dec J and Kleemann W 2000 *J. Phys. D: Appl. Phys.* **33** 1932
[18] Topolov V Yu 2003 *J. Phys.: Condens. Matter* **15** 561
[19] Ganpule C S, Roytburd A L, Nagarajan V, Hill B K, Ogale S B, Williams E D, Ramesh R and Scott J F 2001 *Phys. Rev.* B **65** 014101
[20] Eng L M, Bammerlin M, Loppacher Ch, Guggisberg M, Bennewitz R, Meyer E and Güntherodt H-J 1999 *Surf. Interface Anal.* **27** 422
[21] Tsunekawa S, Ichikawa J, Nagata H and Fukuda T 1999 *Appl. Surf. Sci.* **137** 61
[22] Zhu S and Cao W 1999 *Phys. Status Solidi* a **173** 495
[23] Zhirnov V A 1958 *Zh. Eksp. Teor. Fiz.* **35** 1175
[24] Lawless W N 1968 *Phys. Rev.* **175** 619
[25] Padella J, Zhong W and Vanderbilt D 1996 *Phys. Rev.* B **53** R5969

[26] Zhang X, Hashimoto T and Joy DC 1992 *Appl. Phys. Lett.* **60** 784
[27] Slater J C 1950 *Phys. Rev.* **78** 748
[28] Kinase W, Kobayashi J and Yamada N 1959 *Phys. Rev.* **116** 348
[29] Merz W 1949 *Phys. Rev.* **76** 1221
[30] Lawless W N 1965 *Phys. Rev.* **138** A1751
[31] Kinase W, Ohnishi N, Yoshikawa M and Mori K 1984 *Ferroelectrics* **56** 165
[32] Kinase W, Yoshikawa M and Ohnishi N 1986 *Ferroelectrics* **67** 159
[33] Khatib D, Jullien P and Jannot B 1993 *Ferroelectrics* **145** 181
[34] Kinase W and Mori K 1980 *Ferroelectrics* **29** 235
[35] Nakamura K and Kinase W 1992 *J. Phys. Soc. Japan* **61** 4596
[36] Chaib H, Khatib D and Kinase W 1999 *Nonlinear Opt.* **23** 97
[37] Chaib H, Toumanari A, Khatib D and Kinase W 1999 *Ferroelectrics* **234** 61
[38] Chaib H, Otto T and Eng L M 2003 *Phys. Rev.* B **67** 174109
[39] Chaib H, Otto T and Eng L M 2002 *Phys. Status Solidi* b **233** 250
[40] Seidel J, Grafström S, Loppacher Ch, Trogisch S, Schlaphof F and Eng L M 2001 *Appl. Phys. Lett.* **79** 2291
[41] Stöckle R M, Suh Doug Y, Deckert V and Zenobi R 2000 *Chem. Phys. Lett.* **318** 131
[42] Strukov B A and Levanyuk A P 1998 *Ferroelectric Phenomena in Crystals* (Berlin: Springer)
[43] Press W H, Teukolsky S A, Vetterling W T and Flannery B P 1997 *Numerical Recipes in Fortran 77: the Art of Scientific Computing* (Cambridge: Cambridge University Press)
[44] Cudney R S, Fousek J, Zgonik M and Günter P 1993 *Appl. Phys. Lett.* **63** 3399
[45] Cao W and Randall C 1993 *Solid State Commun.* **86** 435
[46] Cao W and Cross L E 1991 *Phys. Rev.* B **44** 5
[47] Meyer B and Vanderbilt D 2002 *Phys. Rev.* B **65** 104111
[48] Jia C L, Lentzen M and Urban K 2003 *Science* **299** 870